A First Discussion About Digital Filters for Clustered-OFDM Scheme in PLC Systems

Hugo V. Schettino and Moisés V. Ribeiro

***Abstract*— This work aims to investigate the suitability of finite impulse response and infinite impulse response digital filters for separating the clusters in a clustered Orthogonal Frequency Division Multiplexing schemes for power line communication systems. In this regards, we formulate the mathematical problem associated with issue. In the following, we shortly describe several digital filters that may be useful to fulfill the constraints associated with the problem. Based on numerical results and given digital filter design specifications, we reveal that the Chebyshev Type I and elliptic filters show the best trade of among signal noise ratio, date-rate, computational complexity (number of non-zero multipliers).**

***Keywords*— digital filter, orthogonal frequency division multiplexing, interpolated finite impulse response filter, infinite impulse response filter, power line communication.**

I. INTRODUCTION

The increasing demand for ubiquitousness data communication, which is associated with smart grid, is pushing forward the introduction of novel telecommunication technologies. As a result, the use of power line communication (PLC) systems became a interesting solution, potentially convenient and inexpensive, due to use of the existing electric power grid infrastructures [1]. However, electric power grids infrastructure were not designed to transmit high-frequency and very low-power signals, which occupy a wide frequency bandwidth in comparison with mains signal. Also, the communication medium, which we call PLC channel, is periodically time-varying, frequency and time selective and corrupted by the presence of high-power impulsive noises [2]. Additionally, the signal attenuation increases if frequency and/or distance increases.

In order to deal with the hardness of such communication medium, several techniques, mostly based on orthogonal frequency division multiplexing (OFDM) scheme, have been applied so far. One of this techniques is the clustered-OFDM scheme [3] [4]. In this technique, several OFDM schemes operates in parallel and each frequency band occupied by one of these OFDM schemes is named cluster. The main advantage associated with this clustered-ofdm scheme is that the complexity of physical layer of a PLC modem is a fraction of the computational complexity of a base station. As consequence, the cost of PLC system can be reduced.

As the use of clustered-OFDM scheme for PLC system is a novel subject, there are several issues that must to be addressed. For instance, the development of frequency offset estimation because only the in-phase component is used for both baseband and passband data communication; the development of reduced complexity resource allocation technique that exploits the periodically time-varying behavior of PLC channels; the design of digital filter for both baseband and passband modulation and demodulation at the transmitter and receiver sides, to name a few.

This work discusses the suitability of finite impulse response (FIR) and an infinite impulse response (IIR) digital filters, to separate the signals related to each OFDM schemes that constitute a clustered OFDM scheme and to perform the passband signal modulation in power line communication systems. In this regards, we formulate the mathematical problem associated with this issue. In the following, we shortly describe several digital filters that may be useful to fulfill the constraints associated with the formulated problem. Based on numerical results and given digital filter design specifications, we reveal that the Chebyshev Type I and elliptic filters show the best trade of among signal noise ratio, date-rate, computational complexity (number of non-zero multipliers).

The rest of this paper is organized as follows: Section II formulates the problem, while Section III briefly presents the selected digital filters for the analysis. In sequel, Section IV discusses the attained results. Finally, concluding remarks are outlined in Section V.

II. PROBLEM FORMULATION

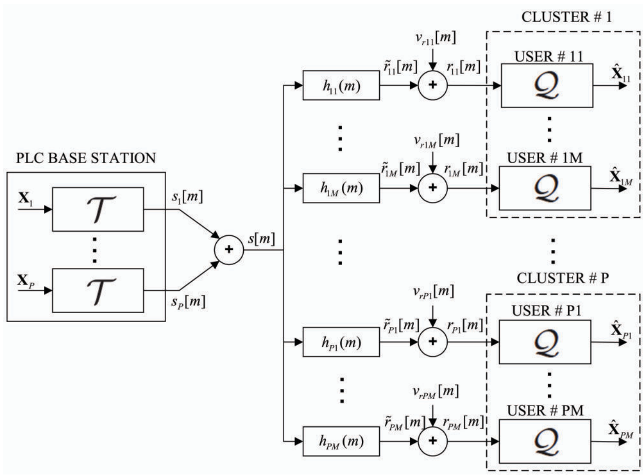

Fig. 1. Clustered HS-OFDM scheme: The downlink data communication direction.

Hugo V. Schettino is with Electrical Engineering Department and Smarti9, Federal University of Juiz de Fora, Juiz de Fora - MG, Brazil. E-mail: hugoschettino@gmail.com. Moisés V. Ribeiro is with Electrical Engineering Department and Smarti9, Federal University of Juiz de Fora, Juiz de Fora - MG, Brazil. E-mail: mribeiro@engenharia.ufjf.br.

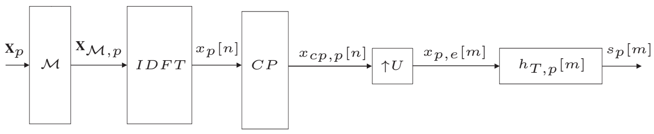

Fig. 2. Block diagram of $\mathcal{T}$.

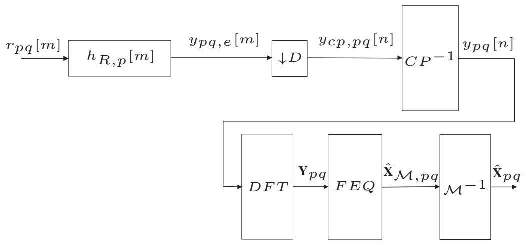

Fig. 3. Block diagram of $\mathcal{Q}$.

Let a clustered hermitian symmetric OFDM (HS-OFDM) scheme in the downlink direction be represented by the block diagram in Fig. 1 [3]. As discussed in [3], the PLC base station makes use of P clusters to communicate with $P \times M$ users when a linear and time invariant PLC channel is considered. A set of distinct M users are allocated to each cluster and each cluster occupies a frequency bandwidth equal to B/P in which B is the total bandwidth available for data communication. Following [3], we know that the transmitter $\mathcal{T}$ and the receiver $\mathcal{Q}$ can be represented by the block diagrams in Figs. 2 and 3, respectively.

At the transmitter, the output of the digital modulation block has an HS-OFDM symbol $\mathbf{X}_p \in \mathbb{C}^{N\times 1}$, in which p denotes the p^{th} cluster, and $N \in \mathbb{Z}_+$ is the number of subcarriers of the HS-OFDM scheme operating in the cluster. $\mathbf{X}_p$ is mapped by the block $\mathcal{M}$ so that $\mathbf{X}_{\mathcal{M},p} \in \mathbb{C}^{2N\times 1}$ and, soon after, it is transformed by the normalized inverse discrete Fourier transform (IDFT). The cyclic prefix is appended to the vector at the output of IDFT ($\mathbf{x}_p \in \mathbb{R}^{2N\times 1}$). The resultant signal is up-sampled by a factor U and filtered by a band-pass, low-pass or high-pass filter ($\mathbf{h}_{T,p} \in \mathbb{R}^{L_{h_{T,p}}\times 1}$, where $L_{h_{T,p}}$ is the transmitter filter length) that chooses one of the clusters for data communication. Finally, the signal $\mathbf{s}_p \in \mathbb{R}^{(2N\times U + L_{cp} + L_{h_{T,p}}+1)\times 1}$, where L_{cp} is the cyclical prefix length, is sent to the digital-to-analog converter.

As can be seen in Fig. 1, the signal of the q^{th} user allocated in the p^{th} cluster is transmitted through a channel impulse response (CIR) represented by $\mathbf{h}_{pq} \in \mathbb{R}^{L_{h_{pq}}\times 1}$, where $L_{h_{pq}}$ is the channel length, and an additive noise $\mathbf{v}_{rpq} \in \mathbb{R}^{(2N\times U + L_{cp} + L_{h_{T,pq}} + L_{h_{pq}}+1)\times 1}$. The signal at the receiver, after the analog-to-digital conversion, is represented by $\mathbf{r}_{pq} \in \mathbb{R}^{(2N\times U + L_{cp} + L_{h_{T,pq}} + L_{h_{pq}}+1)\times 1}$. This signal is filtered by a band-pass, low-pass or high-pass filter impulse response given by vector $\mathbf{h}_{R,p} \in \mathbb{R}^{L_{h_{R,p}}\times 1}$, where $L_{h_{R,p}}$ is the receiver filter length, and, soon after, it is down-sampled by a factor $D = U$. In the following, the cyclic prefix is removed. After that, the normalized discrete Fourier transform (DFT), frequency domain equalization (FEQ) and de-mapping functions are, in this order, applied. The vector $\hat{\mathbf{X}}_{pq} \in \mathbb{C}^{N\times 1}$, is an estimate of the transmitted HS-OFDM symbol that will be submitted to digital demodulation and detection.

If we assume perfect symbol synchronization at the receiver side, then the time domain vectorial representation of the i^{th} received symbol, before the DFT block, by the q^{th} user allocated in the p^{th} cluster is given by

$$\begin{aligned}\mathbf{y}_{pq,i} &= \tilde{\mathbf{y}}_{pq,i} + \sum_{t=0, t\neq p, u\neq q}^{P-1} \tilde{\mathbf{y}}_{tu,i} + \mathbf{C}_{h_{R,p}} \mathbf{v}_{rpq,i} \\ &= \mathbf{C}_{h_{eq,pq}} \mathbf{x}_{p,i} + \sum_{t=0, t\neq p, u\neq q}^{P-1} \mathbf{C}_{h_{eq,tu}} \mathbf{x}_{t,i} + \mathbf{C}_{h_{R,p}} \mathbf{v}_{rpq,i},\end{aligned} \tag{1}$$

in which $\mathbf{y}_{pq,i} \in \mathbb{R}^{2N\times 1}$ refers to the i^{th} received symbol after cyclic prefix removal, which is constituted by $2N$ consecutive samples of $\{y_{pq}[n]\}$; $\tilde{\mathbf{y}}_{pq,i}$, $\tilde{\mathbf{y}}_{tu,i}$ and $\mathbf{v}_{rpq,i}$ denotes the signal received by the q^{th} user allocated in the p^{th} cluster, the interference signal, which is yielded by the u^{th} user in the t^{th} cluster, and the additive noise, respectively; $\mathbf{x}_{p,i}$ is the time domain vectorial representation of the i^{th} HS-OFDM symbol, which is transmitted through the p^{th} cluster; $\mathbf{C}_{h_{eq,pq}} = \mathbf{C}_{h_{R,p}} \mathbf{C}_{h_{pq}} \mathbf{C}_{h_{T,p}}$ is the circulant convolutional matrix for the equivalent channel impulse response $\mathbf{h}_{eq,pq} = [h_{eq,pq}[0],\ h_{eq,pq}[1],\ ...,\ h_{eq,pq}[L_{h_{eq,pq}}-1]]^T$, where $\mathbf{C}_{h_{R,p}}$, $\mathbf{C}_{h_{pq}}$ and $\mathbf{C}_{h_{T,p}}$ denote the circulant convolutional matrices associated with $\mathbf{h}_{R,p}$, $\mathbf{h}_{pq}$ and $\mathbf{h}_{T,p}$. Also, $\mathbf{C}_{h_{eq,tu}} = \mathbf{C}_{h_{Rx,p}} \mathbf{C}_{h_{tu}} \mathbf{C}_{h_{Tx,t}}$.

Note that $\mathbf{h}_{R,p} = [h_{R,p}[0],\ h_{R,p}[1],\ ...,\ h_{R,p}[L_{h_{R,p}} - 1]]^T$, $\mathbf{h}_{pq} = [h_{pq}[0],\ h_{pq}[1],\ ...,\ h_{pq}[L_{h_{pq}} - 1]]^T$, and $\mathbf{h}_{T,p} = [h_{T,p}[0],\ h_{T,p}[1],\ ...,\ h_{T,p}[L_{h_{T,p}} - 1]]^T$ are vectorial representations of $\{h_{R,p}[n]\}_{n=0}^{L_{h_{R,p}}-1}$, $\{h_{pq}[n]\}_{n=0}^{L_{hpq}-1}$, and $\{h_{T,p}[n]\}_{n=0}^{L_{h_{T,p}}-1}$. For the sake of clearness, we state that $\{h_{R,p}[n]\}_{n=0}^{L_{h_{R,p}}-1}$, $\{h_{pq}[n]\}_{n=0}^{L_{hpq}-1}$ and $\{h_{T,p}[n]\}_{n=0}^{L_{h_{T,p}}-1}$ denote the impulse responses of digital filter at the receiver for the p^{th} cluster, PLC channel for the q^{th} user allocated in the p^{th} cluster, and digital filter at the transmitter for the p^{th} cluster, respectively. Additionally, we point out that $L_{cp} \geqslant \max_{p,q} L_{h_{eq,pq}}$, in which L_{cp} is the length of the cyclic prefix and $L_{h_{eq,pq}} = L_{h_{T,p}} + L_{h_{pq}} + L_{h_{R,p}} - 1$.

By applying the DFT in $\mathbf{y}_{pq,i}$, we obtain

$$\begin{aligned}\mathbf{Y}_{pq,i} &= \boldsymbol{\mathcal{F}} \mathbf{y}_{pq,i} \\ &= \tilde{\mathbf{Y}}_{pq,i} + \sum_{t=0, t\neq p, u\neq q}^{P-1} \tilde{\mathbf{Y}}_{tu,i} + \boldsymbol{\mathcal{H}}_{R,p} \mathbf{V}_{rpq,i} \\ &= \boldsymbol{\mathcal{H}}_{T,p} \boldsymbol{\mathcal{H}}_{pq} \boldsymbol{\mathcal{H}}_{R,p} \boldsymbol{\Lambda}_{\sqrt{\boldsymbol{\mathcal{P}}_p}} \mathbf{X}_{p,i} + \\ &\quad \sum_{t=0, t\neq p, u\neq q}^{P-1} \boldsymbol{\mathcal{H}}_{T,t} \boldsymbol{\mathcal{H}}_{tu} \boldsymbol{\mathcal{H}}_{R,p} \boldsymbol{\Lambda}_{\sqrt{\boldsymbol{\mathcal{P}}_t}} \mathbf{X}_{t,i} + \boldsymbol{\mathcal{H}}_{R,p} \mathbf{V}_{rpq,i} \\ &= \boldsymbol{\mathcal{H}}_{eq,pq} \boldsymbol{\Lambda}_{\sqrt{\boldsymbol{\mathcal{P}}_p}} \mathbf{X}_{p,i} + \\ &\quad \sum_{t=0, t\neq p, u\neq q}^{P-1} \boldsymbol{\mathcal{H}}_{eq,tu} \boldsymbol{\Lambda}_{\sqrt{\boldsymbol{\mathcal{P}}_t}} \mathbf{X}_{t,i} + \boldsymbol{\mathcal{H}}_{R,p} \mathbf{V}_{rpq,i},\end{aligned} \tag{2}$$

in which $\boldsymbol{\mathcal{F}} = (1/\sqrt{2N})\mathbf{W}$ and $\mathbf{W} \in \mathbb{C}^{2N\times 2N}$ denotes the $2N$-size DFT matrix, $\boldsymbol{\Lambda}_{\sqrt{\boldsymbol{\mathcal{P}}_p}} =$

$\mathbf{diag}\{\sqrt{\mathcal{P}_p[0]}, \sqrt{\mathcal{P}_p[1]}, ..., \sqrt{\mathcal{P}_p[2N-1]}\}$ because $\mathcal{P}_p[k] = \sqrt{\mathcal{P}_p[k]}\sqrt{\mathcal{P}_p[k]}$ is the power allocated in the k^{th} subcarrier of p^{th} cluster, $\mathbf{tr}(\mathbf{\Lambda}_{\sqrt{\boldsymbol{\mathcal{P}}_p}}\mathbf{\Lambda}_{\sqrt{\boldsymbol{\mathcal{P}}_p}}) = \boldsymbol{\mathcal{P}}_p$, is the transmission power allocated to the p^{th} cluster, $\mathbf{tr}(\cdot)$ is the trace operator, $\boldsymbol{\mathcal{H}}_{T,p} = \mathbf{diag}\{H_{T,p}[0], H_{T,p}[1], ..., H_{T,p}[2N-1]\}$, $\boldsymbol{\mathcal{H}}_{R,p} = \mathbf{diag}\{H_{R,p}[0], H_{R,p}[1], ..., H_{R,p}[2N-1]\}$, $\boldsymbol{\mathcal{H}}_{pq} = \mathbf{diag}\{H_{pq}[0], H_{pq}[1], ..., H_{pq}[2N-1]\}$, $\boldsymbol{\mathcal{H}}_{eq,pq} = \mathbf{diag}\{H_{eq,pq}[0], H_{eq,pq}[1], ..., H_{eq,pq}[2N-1]\}$, $H_{T,p}[k]$, $H_{R,p}[k]$, $H_{pq}[k]$ and $H_{eq,pq}[k]$ is the k^{th} element of $\mathbf{H}_{T,p} = (1/\sqrt{2N})\boldsymbol{\mathcal{F}}[\mathbf{h}_{T,p}^T, \mathbf{0}_{2N-L_{h_{T,p}}}^T]^T$, $\mathbf{H}_{R,p} = (1/\sqrt{2N})\boldsymbol{\mathcal{F}}[\mathbf{h}_{R,p}^T, \mathbf{0}_{2N-L_{h_{R,p}}}^T]^T$, $\mathbf{H}_{pq} = (1/\sqrt{2N})\boldsymbol{\mathcal{F}}[\mathbf{h}_{pq}^T, \mathbf{0}_{2N-L_{h_{pq}}}^T]^T$, and $\mathbf{H}_{eq,pq} = (1/\sqrt{2N})\boldsymbol{\mathcal{F}}[\mathbf{h}_{eq,pq}^T, \mathbf{0}_{2N-L_{h_{eq,pq}}}^T]^T$ respectively; $\mathbf{X}_{p,i} \in \mathbb{C}^{2N\times 1}$ and $\mathbf{V}_{rpq,i} \in \mathbb{C}^{2N\times 1}$ are the frequency domain vectorial representations of the HS-OFDM i^{th} symbol which is transmitted through the p^{th} cluster and the additive noise, respectively.

Let us assume that $\mathbf{X}_{p,i}$ and $\mathbf{V}_{rpq,i}$ are random vectors such that $\mathbb{E}\{\mathbf{X}_{p,i}\} = 0$, $\mathbb{E}\{\mathbf{X}_{p,i} \odot \mathbf{X}_{t,i}\} = \mathbb{E}\{\mathbf{X}_{p,i}\} \odot \mathbb{E}\{\mathbf{X}_{t,i}\}$, $\mathbb{E}\{\mathbf{X}_{p,i}, \mathbf{X}_{p,i}^\dagger\} = \mathbf{\Lambda}_{\sigma^2_{X_p}} = \mathbf{diag}\{\sigma^2_{X_p}(0), \sigma^2_{X_p}(1), ..., \sigma^2_{X_p}(2N-1)\}$, $\mathbb{E}\{\mathbf{V}_{rpq,i}\} = 0$, $\mathbb{E}\{\mathbf{V}_{rpq,i} \odot \mathbf{V}_{rtu,i}\} = \mathbb{E}\{\mathbf{V}_{rpq,i}\} \odot \mathbb{E}\{\mathbf{V}_{rtu,i}\}$, $\mathbb{E}\{\mathbf{V}_{rpq,i}, \mathbf{V}_{rpq,i}^\dagger\} = \mathbf{\Lambda}_{\sigma^2_{V_{rpq}}} = \mathbf{diag}\{\sigma^2_{V_{rpq}}(0), \sigma^2_{V_{rpq}}(1), ..., \sigma^2_{V_{rpq}}(2N-1)\}$, and $\mathbb{E}\{\mathbf{V}_{rpq,i} \odot \mathbf{X}_{t,i}\} = \mathbb{E}\{\mathbf{V}_{rpq,i}\} \odot \mathbb{E}\{\mathbf{X}_{t,i}\}$, in which $\odot$ and $\dagger$ denotes the Hadamard product and complex conjugate operator, respectively. Then,

$$\begin{aligned}&\mathbb{E}\{(\boldsymbol{\mathcal{H}}_{eq,pq}\mathbf{\Lambda}_{\sqrt{\boldsymbol{\mathcal{P}}_p}}\mathbf{X}_{p,i})(\boldsymbol{\mathcal{H}}_{eq,pq}\mathbf{\Lambda}_{\sqrt{\boldsymbol{\mathcal{P}}_p}}\mathbf{X}_{p,i})^\dagger\} \\ &= \mathbf{\Lambda}_{|\boldsymbol{\mathcal{H}}_{eq,pq}|^2}\mathbf{\Lambda}_{\boldsymbol{\mathcal{P}}_p}\mathbf{\Lambda}_{\sigma^2_{X_p}}\end{aligned} \tag{3}$$

where $\mathbf{\Lambda}_{\boldsymbol{\mathcal{P}}_p} = \mathbf{diag}\{\mathcal{P}_p[0], \mathcal{P}_p[1], ..., \mathcal{P}_p[2N-1]\}$, $\mathbf{tr}(\mathbf{\Lambda}_{\boldsymbol{\mathcal{P}}_p}) = \boldsymbol{\mathcal{P}}_p$, $\mathcal{P}_p[k]$ is power allocated to the k^{th} subcarrier of the p^{th} cluster, and

$$\begin{aligned}&\mathbb{E}\{(\sum_{t=0,t\neq p,u\neq q}^{P-1}\boldsymbol{\mathcal{H}}_{eq,tu}\mathbf{\Lambda}_{\sqrt{\boldsymbol{\mathcal{P}}_t}}\mathbf{X}_{t,i} + \boldsymbol{\mathcal{H}}_{R,p}\mathbf{V}_{rpq,i}) \\ &(\sum_{t=0,t\neq p,u\neq q}^{P-1}\boldsymbol{\mathcal{H}}_{eq,tu}\mathbf{\Lambda}_{\sqrt{\boldsymbol{\mathcal{P}}_t}}\mathbf{X}_{t,i} + \boldsymbol{\mathcal{H}}_{R,p}\mathbf{V}_{rpq,i})^\dagger\} \\ &= \sum_{t=0,t\neq p,u\neq q}^{P-1}\mathbf{\Lambda}_{|\boldsymbol{\mathcal{H}}_{eq,tu}|^2}\mathbf{\Lambda}_{\boldsymbol{\mathcal{P}}_t}\mathbf{\Lambda}_{\sigma^2_{X_t}} + \mathbf{\Lambda}_{|\boldsymbol{\mathcal{H}}_{R,p}|^2}\mathbf{\Lambda}_{\sigma^2_{V_{rpq}}}.\end{aligned} \tag{4}$$

Due to the fact that we are using a HS-OFDM scheme, the SNR matrix is given by

$$\mathbf{\Lambda}_{\gamma_{pq}} = \frac{\mathbf{\Lambda}_{|\boldsymbol{\mathcal{H}}_{eq,pq}|^2}\mathbf{\Lambda}_{\boldsymbol{\mathcal{P}}_p}\mathbf{\Lambda}_{\sigma^2_{X_p}}}{\sum\limits_{t=0,t\neq p,u\neq q}^{P-1}\mathbf{\Lambda}_{|\boldsymbol{\mathcal{H}}_{eq,tu}|^2}\mathbf{\Lambda}_{\boldsymbol{\mathcal{P}}_t}\mathbf{\Lambda}_{\sigma^2_{X_t}} + \mathbf{\Lambda}_{|\boldsymbol{\mathcal{H}}_{R,p}|^2}\mathbf{\Lambda}_{\sigma^2_{V_{rpq}}}}, \tag{5}$$

and the multichannel SNR (mSNR) is given by $\gamma_{pq} = \mathbf{det}\big(\mathbf{I}_N + \mathbf{\Lambda}_{\gamma_{pq}}\big)^N - 1$, where $\mathbf{det}(.)$ is the determinant operator and $\mathbf{I}_N$ is N-size identity matrix. Then, we can express the achievable data-rate by

$$R = \max_{\mathbf{\Lambda}_{\boldsymbol{\mathcal{P}}_p}} \frac{2B}{2N + L_{cp}} \sum_{k=0}^{N-1} \log_2(1 + \mathbf{\Lambda}_{\gamma_{pq}}(k,k)) \tag{6}$$

subject to $\mathbf{tr}(\mathbf{\Lambda}_{\boldsymbol{\mathcal{P}}_p}) \leq \boldsymbol{\mathcal{P}}_p$, where B is the frequency bandwidth. Note that the value of L_{cp} may change because the chosen digital filters can results in equivalent impulse responses ($\{h_{eq,pq}[n]\}$) with distinct lengths.

The problem to deal with is to design $\{h_{T,p}[n]\}_{n=0}^{L_{h_{T,p}}-1}$ and $\{h_{R,p}[n]\}_{n=0}^{L_{h_{R,p}}-1}$ such that the achievable date-rate and the mSNR are maximized.

III. Digital Filters

Specifications for designing digital filters for cluster $p = 1$, $p = l$, $l = 2, ..., P-1$, and $p = P$ are showed in Fig. 4-(a) - low-pass filter, Fig. 4-(b) - pass-band filter, and Fig. 4-(c) - high-pass filter, respectively. All digital filters make use of a guard band ω_{gb} to minimize the co-channel interference with its neighboring clusters. The passband ripple and stopband attenuation are denoted by α_p and α_s, respectively. The digital filter of cluster $p = 1$ has a cutoff frequency $\omega_1 = \pi/P$, while cluster $p = P$ has a cutoff frequency $\omega_P = \frac{\pi}{P}(P-1)$. Clusters $p = l$, $l = 2, ..., P-1$, have two cutoff frequencies, $\omega_l^1 = \frac{\pi}{P}(l-1)$ and $\omega_l^2 = \frac{\pi}{P}l$.

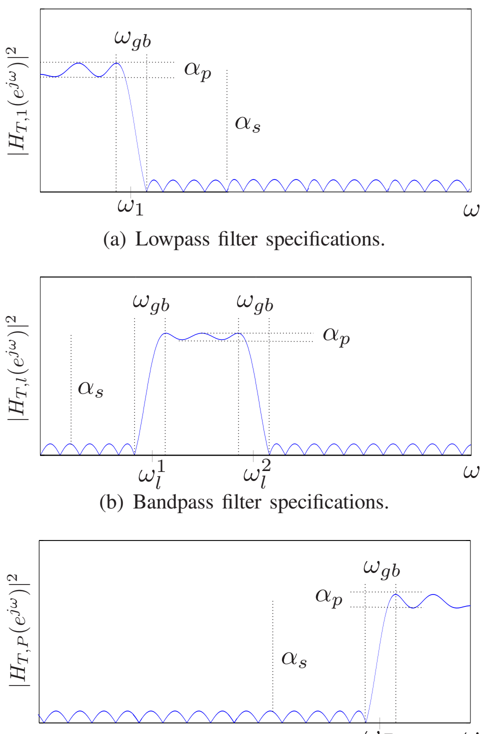

(a) Lowpass filter specifications.

(b) Bandpass filter specifications.

(c) Highpass filter specifications.

Fig. 4. Specications of Digital Filters.

We have chosen the following two FIR digital filters: An equiripple filter and an equiripple Interpolated FIR filter [5] [6]. The equiripple filter was selected due to the stability of the ripple in the passband and stopband [5], and IFIR filter due to the significant savings in terms of number of operations [6]. All chosen FIR digital filters are type-1 and linear phase.

For the sake of comparison, we also have chosen the following four IIR digital filters: Chebyshev Type I, Chebyshev Type II, Butterworth and elliptic. The Chebyshev Type I filter shows a fast roll-off and ripple only in the passband, while Chebyshev Type II offers a fast roll-off and ripple only in the stopband. The Butterworth filter have the passband and stopband frequency response maximally flat and the elliptic filter features an equalized ripple behavior in the passband and the stopband. [5]. These digital filters were chosen because they are the main IIR digital filter considered in the majority of all application and we believe that it is important to verify the gains that they can offer for an clustered-OFDM scheme applied to PLC systems. All the IIR digital filters are designed as a concatenation of 2nd order sections.

IV. Numerical Results

This Section discusses performance analyses related to the use of digital filters, which were described in Section III, in the clustered-OFDM scheme. To analyze the usefulness of the chosen digital filters, we made use of three parameters, γ_{pq}, R, and $L_{h_{eq,pq}}$, these parameters are analyzed in terms of the number of non-zero multipliers of the filters, because it is the operation that demand much more hardware resource. All numerical simulations are carried out in cluster #3 because this cluster suffers interference of the two neighbors clusters. Also, we use of the following constrains to perform the numerical simulations: sampling frequency is $f_s = 100$ MHz; $B = 50$ MHz; up-sampling and down-sampling factors are $U = 5$ and $D = 5$, respectively; $L_{cp} = L_{h_{eq,pq}} + 1$; $P = 5$; $M = 1$; $2N = 1024$, in which N is the number of subcarriers; $\mathbf{\Lambda}_{\mathcal{P}_p} = \mathbf{diag}\{\frac{10^{-1}}{512}, \frac{10^{-1}}{512}, ..., \frac{10^{-1}}{512}\}$; $\mathbf{\Lambda}_{\mathcal{P}_t} = \mathbf{diag}\{\frac{10^{-4}}{512}, \frac{10^{-4}}{512}, ..., \frac{10^{-4}}{512}\}$; $L_{h_{T,p}} = L_{h_{R,p}}$; $\alpha_p = 1.8$ dB, d $\omega_{gb} = 1/50\pi$, and α_s varying to attend the quantity of non-zero multipliers.

To obtain $\{h_{T,p}[n]\}_{n=0}^{L_{h_{T,p}}-1}$ and $\{h_{R,p}[n]\}_{n=0}^{L_{h_{R,p}}-1}$, in the case of IIR filters, the impulse response of the filters are truncated so that the energy of the truncated sequence corresponds to 99% of the energy of the impulse response.

A. AWGN Channel

In this Subsection, we analyze the filters behavior when the clustered-OFDM scheme transmit data through cluster #3, which one we assumed be a additive white Gaussian noise (AWGN) channel, modeled as zero-mean Gaussian random process with noise PSD (Power Spectral Density) $\mathbf{\Lambda}_{\sigma^2_{V_{rpq}}} = \mathbf{diag}\{10^{-3}, 10^{-3}, ..., 10^{-3}\}$. Fig. 5-(a) shows the relation of γ_{pq} while the number of non-zero multipliers of the filters increases. Fig. 5-(b) relates the behavior of achievable date-rate R while the number of non-zero multipliers increases. The filter that obtain an achievable date-rate and a mSNR close to the ideal filter, subject to a low number of non-zero multipliers, is a good candidate. The ideal filter p has $L_{H_{T,p}} = 1$ and $L_{H_{R,p}} = 1$, and the frequency response is equal to one in the all band occupied by the cluster p and zero in the remain band. Fig. 5-(c) associates the $L_{heq,pq}$ with the number of non-zero multipliers. Note that the greater is the number of multipliers, the greater the $L_{heq,pq}$ is. Also, note that R increases with the number of multipliers, until a maximum point, after that L_{cp} begins to influence more than $\mathbf{\Lambda}_{\gamma_{pq}}$ in the value of R and, as consequence, the data-rate is reduced.

If we try to make a decision in favor of a filter we have to come up with the best trade-off among mSNR, achievable date-rate and number of non-zero multipliers. Based on a heuristic approach, we can select Chebyshev Type I and elliptic filters. Note that the Chebyshev Type II attend better achievable data-rate with 57 multipliers, while Chebyshev Type I and elliptic reached close values with 33 multipliers.

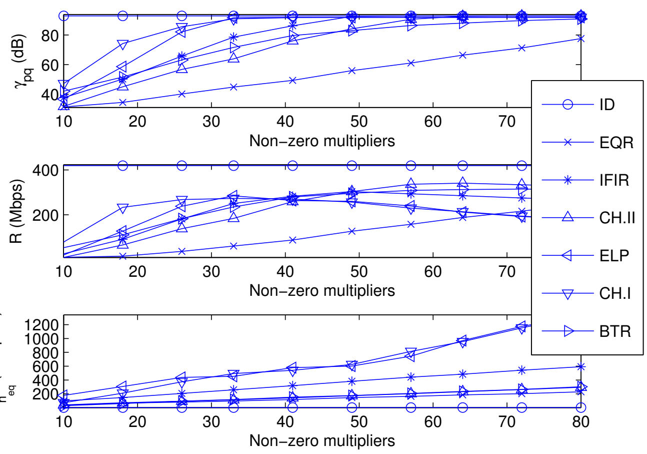

Fig. 5. Analyses of mSNR, achievable date-rate and effective length of the channel with the increase of number of non-zero multipliers of the filters through the AWGN channel.

B. PLC channel

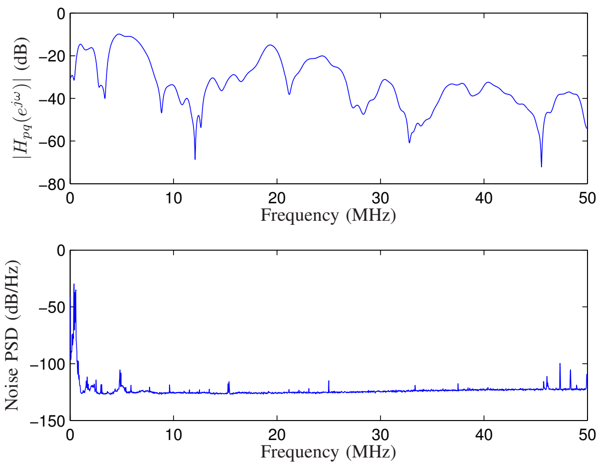

Fig. 6. PLC channel magnitude response and noise PSD.

In this subsection, we use an linear and time invariant indoor PLC channel, which was measured in a house located in Juiz de Fora city to analyze the performance of a clusterd-OFDM scheme. The magnitude response of this PLC channel and the noise PSD are showed in Fig. 6-(a) and 6-(b), respectively.

Fig. 7 shows the same results portrayed in Fig.5, however using a PLC channel. The filter that presented the best trade of among mSNR, achievable date-rate and number of non-zero multipliers is the Chebyshev Type I with 18 multipliers. In second place, the elliptic filter present similar results with 33 multipliers. The Chebyshev Type I filter with 33 multipliers shows a good performance too, leading us to believe that the choice based on AWGN channel is a good option when you do not have PLC channel models to carry out analyses.

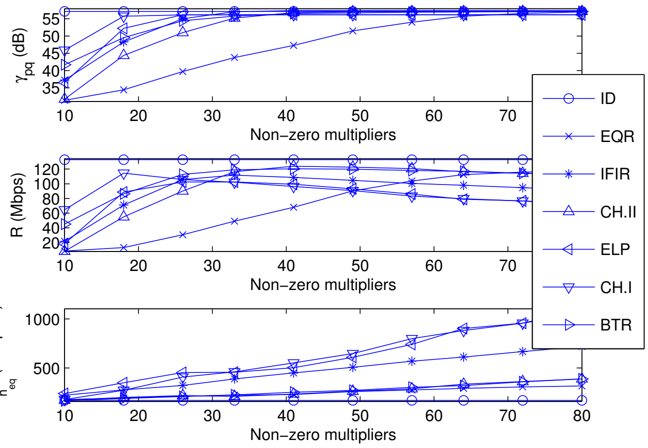

Fig. 7. Analyses of mSNR, achievable date-rate and effective length of the channel with the increase of number of non-zero multipliers of the filters through the PLC channel.

V. Conclusions

This work investigated the use of FIR and an IIR digital filters, with low number of non-zero multipliers, to separate the signals of parallel OFDM schemes that constitute a clustered-OFDM scheme. To do so, the problem associated with the design of digital filters for clustered-OFDM scheme was formulated and several FIR and IIR digital filters were investigated to fulfill the applied constraints.

Based on numerical results and given digital filter design specifications, we noted that the Chebyshev Type I and elliptic filters shows the best trade of among mSNR, achievable date-rate and number of non-zero multipliers.

Acknowledgements

We are thankful for having received financial support from FINEP, FAPEMIG, CNPq, CAPES, P&D ANEEL, CEMIG, INERGE, and Smarti9.

References

[1] Q. Liu and B. Zhao, “Experience of AMR system based on BPL in China,”in *Proc. International Symposium on Power Line Communicatinos and Its Applications*, pp. 280–284, Dresden, Germany, March 2009.

[2] H. C. Ferreira, L. Lampe, J. Newbury and T. G. Swart, *Power Line Communications: Theory and Applications for Narrowband and Broadband Communications over Power Lines*, John Wiley & Sons, 2010.

[3] M. V. Ribeiro, G. R. Colen, F. V. P. Campos, Zhi Quan and H. V. Poor, “Clustered-OFDM for power line communication: When can it be beneficial?,” *IET Communications*, vol. 8, no. 13, pp. 2336–2347, September 2014.

[4] M. V. Ribeiro, F. V. P. de Campos, G. R. Colen, H. V. Shettino, D. Fernandes, L. M. Sirimaco and V. Fernandes, “A novel power line communication system for outdoor electric power grids,” in *Proc. International Symposium on Power Line Communications and its Applications*, Austin, Texas, March 2015.

[5] S. K. Mitra, *Digital Signal Processing: A Computer-Based Approach*, 4^{th} Ed. McGraw-Hill Science, 2010.

[6] Y. Neuvo, C. Y Dong and S. K. Mitra, “Interpolated finite impulse response filters,” *IEEE Transactions on Acoustics, Speech and Digital Signal Processing*, vol. 32, no. 3, pp. 563–570, June 1984.